Available online at www.sciencedirect.com
ScienceDirect
Journal of Power Sources 180 (2008) 330–342
JOURNAL OF POWER SOURCES
www.elsevier.com/locate/jpowsour

On control concepts to prevent fuel starvation in solid oxide fuel cells

Robert Gaynor, Fabian Mueller, Faryar Jabbari, Jacob Brouwer*

National Fuel Cell Research Center, University of California Irvine, Irvine, CA, United States

Received 19 December 2007; received in revised form 26 January 2008; accepted 28 January 2008
Available online 14 February 2008

Abstract

Several methods to prevent fuel starvation in solid oxide fuel cells are developed and investigated. Fuel starvation can occur during transients, if fuel is consumed in the fuel cell faster than it can be supplied by the fuel processing and delivery system. It is demonstrated through simulation that fuel depletion can occur in the fuel cell if no corrective action is employed. Fuel starvation can be prevented by the use of rate limiters, reference governors, and modifications to the fuel-flow controller. The various methods to prevent fuel depletion within the fuel cell are developed and compared. Analysis indicates that reference governors can avoid hydrogen depletion with much less of an impact on transient load following capability than rate limiters. Hence, various reference governors ranging in level of fidelity were developed and compared for performance. It was further demonstrated that with knowledge of the fuel preprocessor response, it is possible to manipulate the fuel flow to minimize reformer flow dynamics, minimizing the need to govern the fuel cell transient capability.

Keywords: SOFC; Dynamic modeling; Fuel flow delay; Reference governor; Flow compensation; Loop shaping

1. Introduction

Fuel cell systems with fast load following capabilities offer increased flexibility over systems with limited transient capability. A fast fuel cell system will allow use in a larger number of applications and can also limit the undesirable dynamics put onto the utility grid, which often is an important barrier to greater fuel cell adoption [1]. Various control concepts to prevent hydrogen starvation that result in different transient capabilities are investigated herein. This investigation identifies methods for implementing advanced controls to improve fuel cell transient capability without making major hardware changes, and provides fuel cell designers a basis to evaluate controller cost benefits and risks in commercial systems.

The ability of a fuel cell to track load demands is limited by several constraints (e.g., maximum fuel cell temperature, minimum fuel cell voltage), which can permanently damage the system if they are violated. Thus, in order to develop load following fuel cells several constraints need to be considered during the physical system design and control system design. Some of these constraints can be managed by the use of fixed filters or rate limiters to prevent the input signals from changing too rapidly. However, this approach requires that the limits be set for the worst-case scenario, which can result in a slow or sluggish response.

Reference governors are an alternative that can improve the response of the system while still preventing constraint violations, by reducing the reference/command signal when a constraint violation is likely [2]. Since a reference governor only acts when needed, the system response can be improved compared to rate limiters or delays, by avoiding artificial and conservative limits imposed by the worst case. This becomes even more important when several different constraints are present, since often a worst-case combination is used for safe operation, increasing the 'sluggishness' of the response significantly.

A predictive reference governor will use a system model to calculate the reference command by predicting the future response of the system. The complexity of the model used will affect both the computational requirements and performance of the reference governor. The reference governor calculations must be accomplished in finite and reasonable time, which necessitates the selection of a prediction horizon that can also

* Corresponding author. Tel.: +1 949 824 1999; fax: +1 949 824 7423.
E-mail addresses: rmg@nfcrc.uci.edu (R. Gaynor), fm@nfcrc.uci.edu (F. Mueller), fjabbari@uci.edu (F. Jabbari), jb@nfcrc.uci.edu (J. Brouwer).

0378-7753/$ – see front matter © 2008 Elsevier B.V. All rights reserved.
doi:10.1016/j.jpowsour.2008.01.078

Nomenclature

C_v	specific heat (kJ kg^{-1} K^{-1})
F	Faraday's constant (96,487 C mol^{-1})
Δgf^0	change in Gibbs free energy at standard state (kJ kmol^{-1})
h	enthalpy (kJ kmol^{-1})
i	current density (A m^{-2})
I	current (A)
k	orifice constant (kPa s^2 kmol^{-1})
n	number of electrons in reaction
N	number of moles in control volume (kmol)
$\dot{N}$	molar flow rate (kmol s^{-1})
P	pressure (kPa)
Pw	power (kW)
Pwd	power demand (kW)
$\dot{Q}$	heat transfer (kW)
r	reaction rate
R	universal gas constant (8.3145 kJ kmol^{-1} K^{-1})
SA	surface area of electrode (m^2)
T	temperature (K)
U	utilization
v	voltage loss (V)
V	volume (m^3); voltage (V)
$\dot{W}$	work (kW)
x	species mole fraction
$\dot{x}$	rate of change of species mole fraction (s^{-1})

Greek letters

λ	eigenvalue
ρ	density of electrolyte (kg m^{-2})

Subscripts

act	activation loss
con	concentration loss
fc	fuel cell/flow entering fuel cell
in	inlet
I	chemical component
max	maximum allowable value
min	minimum allowable value
ohm	ohmic loss
out	outlet
ref	reformer/flow entering reformer
0	nominal state

affect the computational requirements and performance of the reference governor.

Several constraints that can limit the response of fuel cell systems have been identified in literature on fuel cell system dynamics. These constraints include hydrogen starvation, oxygen starvation, turbo machinery choke/surge, temperature/temperature gradient, steam to carbon ratio, and burner backflow. For example, in Vahidi et al. [3] the proton exchange membrane (PEM) fuel cell system is limited by oxygen starvation in the cathode and choke and surge of the compressor. While oxygen starvation can be a problem in PEM systems during power increases since the air is limited to minimize the parasitic losses, in high temperature fuel cells oxygen starvation is less likely to occur because the airflow is significantly above the stoichiometric value in order to cool the fuel cell stack. In cases where the oxidizer pressure increases faster than the anode compartment pressure backflow may be a problem. This type of constraint lowered the system response of the hybrid system presented in Stiller et al. [4], which was further described in Stiller et al. [5].

This paper focuses on the fuel starvation constraint since this constraint will affect all solid oxide fuel cell (SOFC) systems regardless of the specific configuration, and is considered a key and fundamental limiting factor in power following [6]. During power transients, fuel starvation can be a problem if the current consumes electrochemically active fuel constituents more rapidly than the fuel supply system can provide them. The rate at which electrochemically active fuel constituents (primarily hydrogen) can be supplied is determined by the dynamics of the fuel preparation system, which include fluid flow, thermal response, and chemical kinetics in the fuel processor and fuel cell. These considerations, naturally, also depend on the types of valves, sensors and reformer system employed.

Beckhaus et al. [7] considers the dynamics of a steam reformer for a PEM system, by modeling the chemical kinetics and fluid dynamics separately. The system is modeled as a series of control volumes for each of the reactors, with flow restrictions modeled by plenum and flow restriction equations used to model the fluid flow dynamics. The decoupling of the fluid and chemical dynamics is accomplished by assuming constant temperatures and reaction rates in each of the control volumes. Tsourapas et al. [8] examines the hydrogen starvation problem for a PEM fuel cell system that uses partial oxidation reactions and water gas shift reactions to produce hydrogen for the fuel cell. The authors also developed a controller to correct hydrogen starvation and conducted a system-wide optimization analysis to determine the optimal fuel and airflow rates into the fuel processor system.

The problem of hydrogen starvation needs constraint management techniques such as reference governors. Currently, much of the literature on reference governors for fuel cell systems has focused on PEM fuel cell systems. Sun and Kolmanovsky [2] have developed a reference governor to prevent oxygen starvation in a PEM fuel cell system. In their approach the current is limited in order to prevent oxygen starvation in the system. The reference governor calculates the maximum allowable current for each time interval by use of the bisection method. The model used to calculate the allowable current demand assumes that the temperature and humidity are controlled at their set-point values.

In Vahidi et al. [9] model predictive control was used to prevent oxygen starvation in a PEM system that uses an ultracapacitor to meet any current demand that could not be met by the fuel cell. The model predictive controller assumes constant disturbances over the time horizon and optimizes the distribution between the current demand met by the fuel cell and ultracapacitor over this time horizon. Vahidi et al. [3] compared two

reference governors that can prevent both oxygen starvation and compressor choke and surge for a PEM fuel cell system. One reference governor uses model predictive control to modify the current demand in order to prevent these constraints; the other uses a fast reference governor approach, explained in [10], to prevent constraint violations.

While the use of reference governors has been developed for use in PEM systems, the use of reference governors in SOFC systems has remained unexplored. Differences in the temperature, airflow, and fuel processor requirements will result in significantly different constraint management requirements for PEM and SOFC systems. The goal of this paper is to show how different approaches for reference governor design can prevent constraint violations in SOFC systems while improving the dynamic performance characteristics of the system. First, reference governors are developed for a simplified model of the fuel cell system that runs on pure hydrogen. The reference governors are then modified for use in a more realistic model that uses natural gas reformation to supply the hydrogen. While constraints related to the airflow such as fuel cell and combustor temperature must also be considered during system transients, these issues are not considered in this work. The management of these constraints will result in tradeoffs between the net power output and the airflow rate. Previous work indicates that a properly designed airflow controller can minimize its impact on load following while still maintaining the system thermal requirements since the characteristic thermal response time is larger than characteristic fluid flow response times [6]. The focus of the paper is on the limiting nature of fuel (hydrogen) starvation in power following applications.

2. Model description

Matlab-Simulink® was used to create the current dynamic models used to determine how system constraints will affect the load following ability of SOFC systems. The modeling methodology used herein has been previously developed in [11–14], and compared favorable to experimental testing of dynamic single cell transients [15], integrated simple cycle SOFC systems [16], SOFC-MTG hybrid systems [17], and PEM stationary fuel cell systems [18]. The modeling methodology has further been used to investigate control of SOFC system in [6,11,16,19–21].

In brief, this technique involves discretizing each component into control volumes. Within each gas control volume species mole fractions and temperatures are dynamic states determined from transient species and energy conservation equations, respectively. Temperature is the dynamic state of each solid control volume, which is derived from the transient energy conservation equation. The pressure is also a dynamic state for large plenum volumes derived from the choked flow equation and the ideal gas law. In addition, the shaft angular speed of blowers and/or compressors in such systems is an additional dynamic state derived from conservation of momentum equation associated with the modeled blower or turbo-machinery. This section provides a brief overview of the dynamic equations and modeling method used in this work.

The species mole fractions at each gas node are calculated from species conservation as follows:

$$\frac{\mathrm{d}(Nx_i)}{\mathrm{d}t} = \dot{N}_{i\_\mathrm{in}} + r_i - x_i\dot{N}_{\mathrm{out}} \tag{1}$$

where x_i is the mole fraction of species i, $\dot{N}_{i\_\mathrm{in}}$ the molar flow rate of species i entering the control volume, r_i the reaction rate of species i, $\dot{N}_{\mathrm{out}}$ the total molar flow rate leaving the control volume, and N is the total number of moles in the control volume.

The temperature of each gas control volume is determined from energy conservation by the following equation:

$$NC_{\mathrm{V}}\frac{\mathrm{d}T}{\mathrm{d}t} = \dot{N}h_{\mathrm{in}} - \dot{N}h_{\mathrm{out}} + \dot{Q}_{\mathrm{in}} - \dot{W}_{\mathrm{out}} \tag{2}$$

where h_{in} is the enthalpy of the inlet stream, h_{out} the enthalpy of the exit stream, $\dot{Q}_{\mathrm{in}}$ the heat transferred top the control volume, $\dot{W}_{\mathrm{out}}$ the work done by the control volume, and C_{v} is the specific heat of the gas.

The change in pressure of a plenum volume can be derived from the ideal gas law and is determined by the following equation:

$$\frac{\mathrm{d}(P/T)}{\mathrm{d}t} = \frac{R}{V}(\dot{N}_{\mathrm{in}} + \sum r - \dot{N}_{\mathrm{out}}) \tag{3}$$

where R is the universal gas constant, T the temperature of the control volume, and V is the volume of the control volume.

A three-control volume bulk model was used to model the dynamics of the fuel cell stack. The three control volumes are the anode bulk gas, cathode bulk gas, and electrolyte tri-layer (bulk). While the bulk model does not capture spatial temperature or species variations, bulk models provide adequate estimation of the system response [12,22]. The temperature and species mole fractions are resolved for the cathode and anode gas streams and the temperature is resolved for the solid electrolyte tri-layer. Convective heat transfer occurs between the electrolyte tri-layer and the cathode and between the electrolyte tri-layer and the anode. Radiation heat transfer occurs between the tri-layer and the interconnect.

For systems with indirect internal reformation, a separator plate between the anode compartment and the reformer compartment was added. Conduction between the separator plate and the electrolyte tri-layer was added to simulate the conduction that will occur along the supports between the separator plates and the electrolyte.

The reaction rates of the species in the anode are a result of the electrochemical and reformation reactions. The reactions rates in the cathode gas stream are a result of the electrochemical reactions. The reactions rates associated with the reformation reactions are the same as used in [6,11,12] (from Xu and Froment [23,24]). The reaction rates associated with the electrochemistry can be determined from the fuel cell electrical current and Faraday's law.

$$r_{\mathrm{H_2}} = -\frac{i\,\mathrm{SA}}{2F}, \qquad r_{\mathrm{H_2O}} = \frac{i\,\mathrm{SA}}{2F}, \qquad r_{\mathrm{O_2}} = -\frac{i\,\mathrm{SA}}{4F} \tag{4}$$

where i is the current density, SA the surface area of the electrode, and F is Faraday's constant.

The voltage and power produced by the fuel cell can be determined from the system states through the Nernst equation and voltage polarizations.

$$V = -\frac{\Delta g f^0}{2F} + \frac{RT_{fc}}{2F} \ln\left[\frac{x_{H_2} x_{O_2}^{1/2}}{x_{H_2O}} P_{fc}^{1/2}\right] - v_{act} - v_{ohm} - v_{conc} \quad (5)$$

where $\Delta g f^0$ is the change in Gibbs free energy, T_{fc} the temperature of the fuel cell electrolyte, x_{H_2} the hydrogen mole fraction in the anode, x_{H_2O} the water mole fraction in the anode, x_{O_2} the oxygen mole fraction in the cathode, P_{fc} the pressure of the cathode and anode gas streams, and v_{act}, v_{ohm}, and v_{conc} are the activation, ohmic, and concentration losses, respectively.

The power produced by the fuel cell can be calculated by multiplying the voltage by the current.

$$Pw = I\left(-\frac{\Delta g f^0}{2F} + \frac{RT_{fc}}{2F} \ln\left[\frac{x_{H_2} x_{O_2}^{1/2}}{x_{H_2O}} P_{fc}^{1/2}\right] - v_{act} - v_{ohm} - v_{conc}\right) \quad (6)$$

where I is the total current produced by the fuel cell.

The reformer gas stream is modeled as a single control volume. The species mole fractions, temperature, and pressure are resolved within the reformer volume and heat transfer occurs between reformer volume and the separator plate. Chemical kinetics within the reformer are modeled as in the fuel cell. The flow rate leaving the reformer and entering the anode is determined by the pressure difference across the flow restriction.

$$\dot{N}_{fc} = \sqrt{\frac{P_{ref} - P_{fc}}{k}} \quad (7)$$

where P_{ref} is the pressure of the reformer control volume and k is the orifice constant.

The orifice equation can be derived form the Bernoulli equation and is valid for incompressible flows, which is the case for flows throughout the fuel cell system. The flow restriction equation has been used in other fuel reformation models [6–8]. This equation has also been validated for use in simulating reformation systems by Beckacaus et al. [7].

3. Fuel cell system controls

A fuel cell system will require a control system in order to maintain the system operating requirement and to track loads during operation. A general method for controlling fuel cell systems has been identified in the literature [4,14,22], where the airflow rate is used to control the fuel cell temperature, the fuel flow rate is used to control the utilization, and the current is used to control the power. Fig. 1 illustrates the general control system used in the current work. The fuel flow rate that will result in the desired utilization can be calculated from the current and controlled with a feed forward term.

$$\dot{N}_{ref} = \frac{i\,SA}{2FU} \quad (8)$$

where U is the desired utilization.

The airflow rate is controlled by manipulating the blower power. A feed forward term is generally required for the blower power control due to the slow temperature response of the stack. The current is manipulated by the power electronics in order to produce the load power demand and the power required by the fuel cell parasitic loads (primarily the blower). In the simulations integral feedback is used to manipulate the current in order to control the total power produced from the fuel cell.

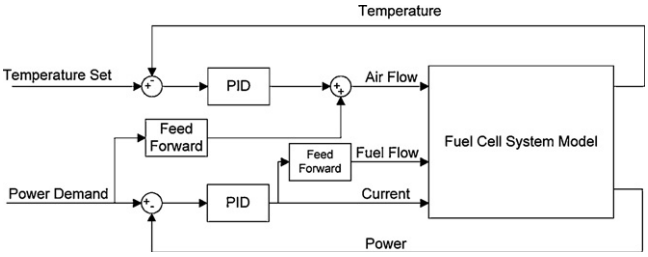

Fig. 1. Illustration of the fuel cell system control structure.

4. Simplified model of fuel depletion

Fuel starvation can occur if the fuel cell consumes electrochemically active species faster than they can be supplied by the fuel reformation system. If the anode becomes fuel starved, no power will be produced by the stack and the stack could be permanently damaged as the material in the anode becomes oxidized.

Insight into the cause and potential solutions to the fuel starvation problem can be gained by first considering a simplified version of the problem. In the current work, hydrogen is assumed to be the only electrochemically active species. Hydrogen starvation can be modeled in a simplified fashion by considering a fuel cell that runs on pure hydrogen with a first order delay in the fuel flow entering the anode compartment. The model can then be simplified to a second order system of equations by neglecting the temperature dynamics of the fuel processing system, the electrolyte tri-layer and the anode gas stream. This assumption is reasonable considering the fact that the thermal response of the fuel cell is much slower than the fluid flow, chemistry and electrochemistry responses of the system [6]. If constant oxygen utilization is also assumed then the power output of the system can be calculated from the hydrogen mole fraction and current.

With these assumptions the reformer exit pressure can be evaluated as

$$\dot{P}_{ref} = \frac{RT_{ref}}{V_{ref}}(\dot{N}_{ref} - \dot{N}_{fc}) \quad (9)$$

where the reformer exit flow rate ($\dot{N}_{fc}$) is evaluated from the orifice flow equation (Eq. (7)). By assuming a constant number of moles in the anode control volume, the fuel cell exit mole fraction can then be determined from species conservation as

$$\dot{x}_{H_2} = \frac{\dot{N}_{fc} - (i\,SA/2F) - x_{H_2}\dot{N}_{fc}}{N} \quad (10)$$

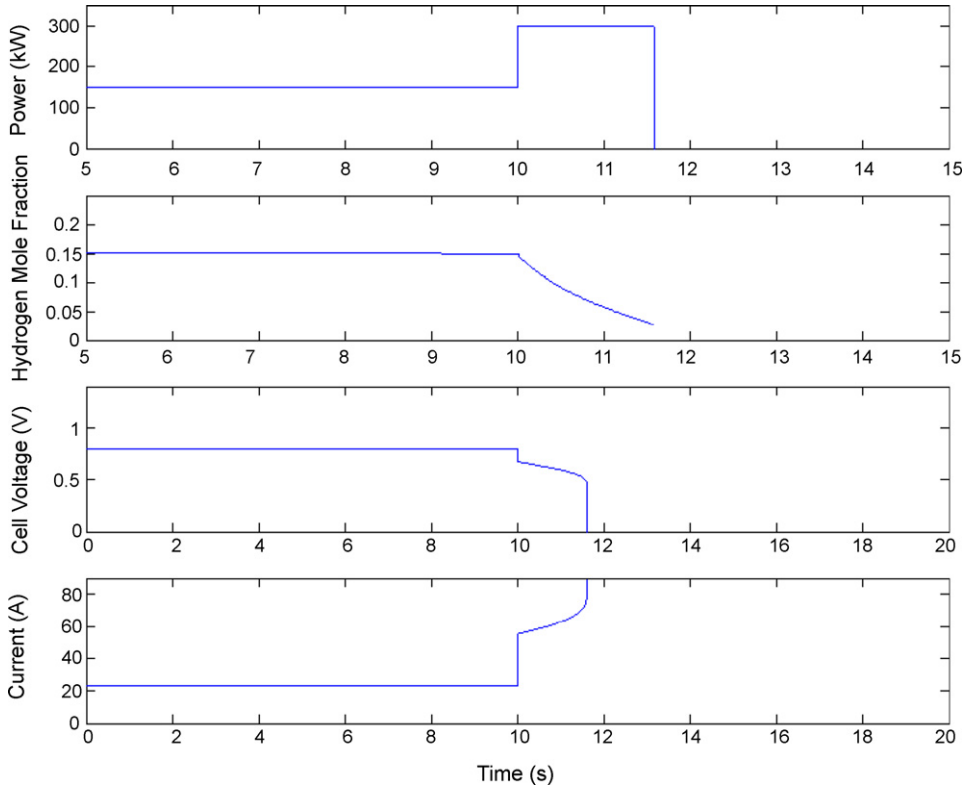

Fig. 2. Response of power, hydrogen mole fraction, cell voltage, and current for a 250 kW step change in power demand with no reference governor.

The power produced by the fuel cell can be calculated from current and fuel cell exit hydrogen mole fraction.

$$\mathrm{Pw} = I\left(-\frac{\Delta g f^0}{2F} + \frac{RT_{\mathrm{fc}}}{2F}\ln\left[\frac{x_{\mathrm{H_2}} x_{\mathrm{O_2}}^{1/2}}{1 - x_{\mathrm{H_2}}} P_{\mathrm{fc}}^{1/2}\right] - v_{\mathrm{act}} - v_{\mathrm{ohm}} - v_{\mathrm{conc}}\right) \quad (11)$$

5. Fuel depletion analysis

In order to demonstrate the potential for fuel starvation, Fig. 2 shows the response of the simplified system with a maximum power output of 350 kW using the proposed control structure for a 250 kW step increase in power demand from 50 to 300 kW with the parameters shown in Table 1. The hydrogen stored in the anode volume allows the system to produce the demanded power for about a second before the hydrogen is nearly depleted as the system cannot deliver hydrogen fast enough to replenish the consumed hydrogen due to the fuel flow delay. The low hydrogen mole fraction causes the voltage to decline sharply, which causes the power produced by the fuel cell to drop. Consequently, the fuel cell power feedback controller tries to increase the current to meet power demand, which exacerbates the problem. Since current is proportional to hydrogen consumption, the fuel cell current must be limited such that the hydrogen within the fuel cell does not become depleted.

Table 1
System parameters

Parameter	Value
Set utilization	0.85
Max utilization	0.9
Fuel cell temperature	1150 K
Anode volume	1.0×10^{-4} m^3
Reformer volume	1 m^3
Reformer orifice constant	1.5×10^6 kPa/(kmol s)^2
Reformer temperature	650 K

6. Fuel starvation prevention

Four general methods were considered for fuel starvation prevention. The first method was the use of a rate limiter on the power demand signal on a system with current-based feed forward control of the fuel flow. The second method considered was to use a fuel cell power reference governor with only a reformer model. The third method was to use a fuel cell power reference governor with both a reformer and fuel cell hydrogen depletion model to improve the performance of the system by considering the hydrogen storage in the anode compartment. Finally, the use of fuel flow compensation to reduce the flow delay was considered as a method for improving the load following ability of the system. By estimating the reformer response, it is possible to control the reformer fuel flow, to shape the reformer response, avoiding hydrogen depletion in the fuel cell. The reference governors are first developed based on the simplified hydrogen starvation analysis. Modifications required to allow these reference governors to work with a system using natural gas reformation are then explained and demonstrated.

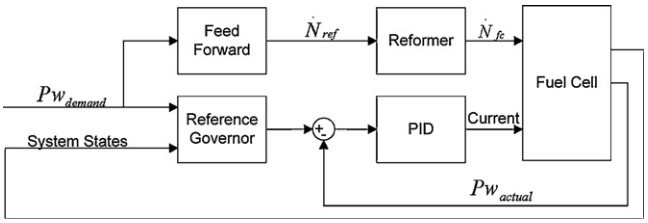

Fig. 3. Power reference governor control structure.

6.1. Rate limiter

One way to prevent hydrogen depletion from occurring is to use a rate limiter on the power demand. The value of the rate limiter should be selected so that the hydrogen mole fraction will never go below its minimum value for the worst-case scenario, which occurs when the power demand increases from the minimum to the maximum system output. While the rate limiter is relatively simple to implement it is not an ideal solution for two reasons. First, the rate limiter will slow the power output even when the hydrogen would not have been depleted. Secondly, the rate limiter will increase the time it takes the fuel to reach the fuel cell since the rate limiter will also limit the fuel flow command.

6.2. Fuel cell power reference governor

A faster load following response can be obtained by implementing a fuel cell power reference governor to avoid hydrogen depletion in the fuel cell. The general fuel cell power reference controller considered is illustrated in Fig. 3. The goal of the fuel cell power reference governor is to find the maximum value of the power demand that will not cause a violation of the minimum hydrogen mole fraction constraint. A system model is required to calculate the maximum feasible power demand. The performance of the reference governor depends on the complexity of the model used as well the time horizon used for the calculation. The variations considered for the reference governor model are described in this section.

6.2.1. Reference Governor A (governor with reformer model)

In the simplest case the reference governor model can be simplified to the single state of Eq. (9) representing the reformer pressure. The reference governor model constants and initial conditions are measured directly from the system. From the reformer pressure the reformer flow rate can be evaluated from the orifice flow equation. With the reformer flow rate, the maximum current can then be evaluated as

$$I_{\max} = \frac{2F(1 - x_{\mathrm{H_2min}})\dot{N}_{\mathrm{fc}}}{\mathrm{SA}} \tag{12}$$

where $x_{\mathrm{H_2min}}$ is the minimum allowable hydrogen mole fraction.

This equation represents the maximum current such that a minimum fuel cell hydrogen mole fraction is maintained at steady state. Under these assumptions the calculation for determining the maximum output are simplified but the performance will be suboptimal since the hydrogen stored in the anode is not accounted for by this reference governor calculation.

Fig. 4 shows how the maximum current can be used to modify the power demand signal to prevent hydrogen starvation. In this configuration the reference governor determines the maximum current based on the system states. A feedback controller with large gains is then used to set the power demand to a value that will prevent the current from exceeding its maximum value. A negative rectifier is used so that the reference governor will only be active if the current will exceed its maximum value.

6.2.2. Reference Governor B (governor with both reformer and fuel cell model)

Accounting for both the reformer flow dynamics and stored hydrogen within the fuel cell anode can improve the performance of the reference governor but will result in greater computational requirements. When the anode dynamics are also considered, the reference governor model will need to simulate the response of the hydrogen mole fraction due to a change in the power demand. This problem is formulated as a constrained maximum where the goal is to find the maximum $\beta \in [0,1]$ such that the hydrogen mole fraction constraint is not violated:

$$\mathrm{Pw}(k+1) = \mathrm{Pw}(k) + \beta(\mathrm{Pwd} - \mathrm{Pw}(k)) \tag{13}$$

where $\mathrm{Pw}(k)$ is the amount of power currently being produced by the fuel cell and Pwd is the total power demand.

The general procedure for this reference governor that is used to prevent hydrogen starvation is illustrated in Fig. 5. At each time step the calculation begins by using the system states and power demand, which is assumed to remain constant, as inputs into the reference governor model to predict the reformer flow rate and estimate the amount of hydrogen within the anode compartment over a time horizon. If the model predicts no constraint violation over the time horizon, then the β equals one and the fuel cell tracks the power demand. However, if the model predicts that the minimum hydrogen mole fraction constraint will be violated then the reference governor selects a new power based

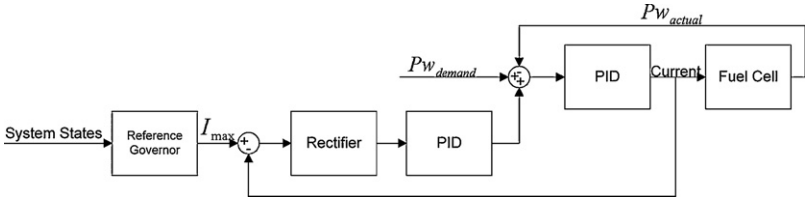

Fig. 4. Control structure of current-based reference governor.

on the procedures of the bisection method. This procedure is repeated until the maximum permissible output is found or the power demand is tracked.

In order to predict the hydrogen mole fraction over the required time horizon, a nonlinear model of the system can be constructed of the system from Eqs. (9)–(11). In this model the current is used to control the power output. Since the electrochemical response of the fuel cell is much faster than the reformer dynamics, a model where the current is used to control the power can be obtained by solving Eq. (11) for the current that will produce the desired power demand. The reference governor will then use the procedure mentioned previously with a differential equation solver to find the maximum allowable power that will not cause hydrogen starvation.

A linear approximation of the model, described previously, can also be used for the reference governor model, which can reduce the computational requirement of the reference governor. The linear system with the control structure presented in Fig. 3 (neglecting the airflow controller) can be described as follows:

$$\begin{bmatrix} \delta\dot{P} \\ \delta\dot{x}_{\mathrm{H_2}} \end{bmatrix} = \begin{bmatrix} -\dfrac{RT_{\mathrm{ref}}}{V_{\mathrm{ref}}2\sqrt{P_0 k}} & 0 \\ \dfrac{1-x_0}{2N\sqrt{P_0 k}} & -\dfrac{\sqrt{P_0}}{\sqrt{kN}} + \dfrac{(\partial \mathrm{Pw}/\partial x_{\mathrm{H_2}})\delta x_{\mathrm{H_2}}}{(\partial \mathrm{Pw}/\partial I)} \end{bmatrix} \times \begin{bmatrix} \delta P \\ \delta x_{\mathrm{H_2}} \end{bmatrix} + \begin{bmatrix} \dfrac{RT_{\mathrm{ref}}}{V_{\mathrm{ref}}} & 0 \\ 0 & -\dfrac{1}{N2F(\partial \mathrm{Pw}/\partial I)} \end{bmatrix} \begin{bmatrix} \delta\dot{N}_{\mathrm{ref}} \\ \delta \mathrm{Pw} \end{bmatrix} \tag{14}$$

where x_0 is the nominal hydrogen mole fraction and P_0 is the nominal pressure.

The nominal states for the linearization calculation are the states at time k, while the nominal inputs are the values that correspond to the nominal inputs at steady state. Differences between the linear dynamics and the actual system dynamics will compromise the ability of the reference governor to accurately predict the response of the system. Errors that cause the reference governor to overestimate the maximum power will prevent the reference governor from avoiding constraint violation and therefore need to be accounted for in the linear model. The two major sources of these errors come from the linearization of the reformer flow (Eq. (9)) and power (Eq. (11)) equations. The eigenvalue that determines the dynamics of reformer flow can be determined from inspection of the linear system and related to the steady state flow rate as follows:

$$\lambda_1 = -\frac{RT_{\mathrm{ref}}}{V_{\mathrm{ref}}2\dot{N}_{\mathrm{ref}}k} \tag{15}$$

As the flow rate becomes larger the absolute value of this eigenvalue becomes smaller, which results in a slower system response. This error will cause the reference governor to assume a faster response for the hydrogen flow than actually occurs, causing the reference governor to over predict the maximum allowable power. This problem can be overcome by adjusting the value of this eigenvalue in order to account for the slower dynamics at higher flow rates.

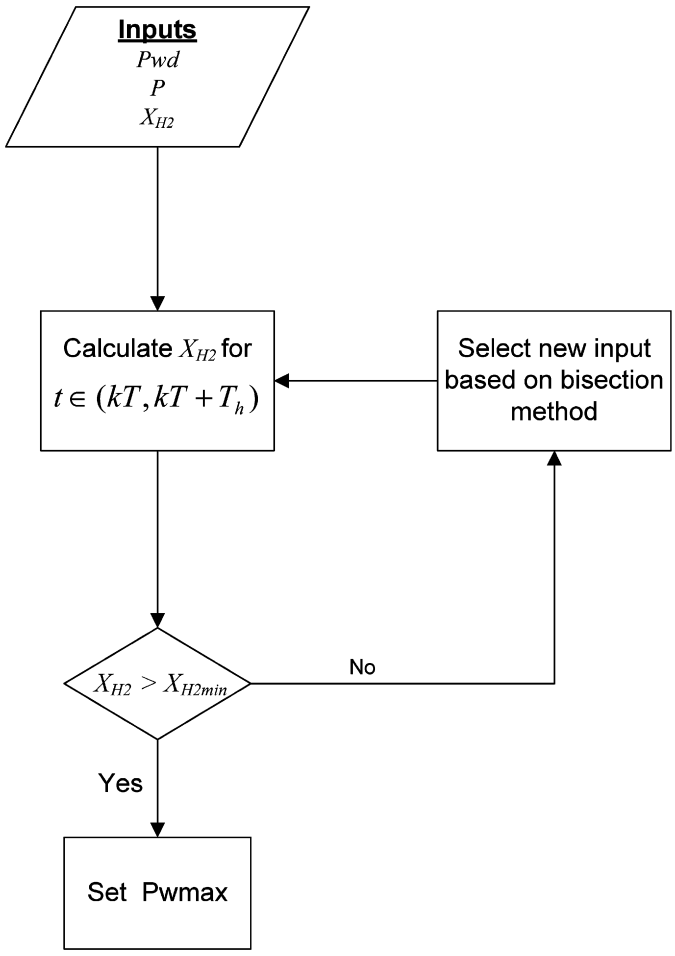

Fig. 5. General procedure for reference governor calculations.

The other major source of error is due to the partial derivative of power with respect to current term ($\partial \mathrm{Pw}/\partial I$) in the linearization of the power Eq. (11). This term is dependent on the nominal hydrogen mole fraction. In the linear model this term determines how much the current must change in order to produce the desired power, which also determines how much hydrogen will be consumed. This term is dependent on the hydrogen mole fraction. At lower hydrogen mole fraction values, a larger amount of current is required to produce the same amount of power. Using the current value of the hydrogen mole fraction will cause the reference governor to over predict the maximum allowable power. Using the minimum hydrogen mole fraction instead can prevent the over prediction of the maximum power since the ($\partial \mathrm{Pw}/\partial I$) term used in the linear model will always be higher than the actual value.

The selected time horizon can also affect the performance and computational requirements of the reference governors. As the time horizon approaches zero the reference governor will respond to the current value of the hydrogen mole fraction. The voltage of the fuel cell can be used as a measure of the mole fraction through the Nernst and polarization equations. A voltage based reference governor can be constructed in a manner similar to the current-based reference governor shown in Fig. 4. However, the voltage-based reference governor calcu-

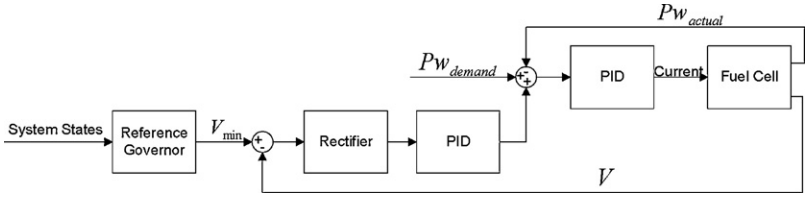

Fig. 6. Control structure of voltage-based reference governor.

lates the minimum voltage instead of a maximum current. An illustration of the voltage-based reference governor is shown in Fig. 6.

The minimum voltage can be found by substituting the minimum hydrogen mole fraction into Eq. (5).

$$V_{\min} = -\frac{\Delta g f^0}{2F} + \frac{RT_{\rm fc}}{2F} \ln\left[\frac{x_{\rm H2min} x_{\rm O_2}^{1/2}}{1 - x_{\rm H2min}} P_{\rm fc}^{1/2}\right] - v_{\rm act} - v_{\rm ohm} - v_{\rm conc} \quad (16)$$

6.3. Reference Governor C (w/flow compensation)

Since the power demand response of the fuel cell is limited by the rate at which fuel can be supplied to the fuel cell, using a fuel-flow controller that will send additional fuel can increase the transient capability of the system. In an actual system, the ability to increase the fuel flow will be limited by the maximum fuel flow rate of the system. In this work the maximum fuel flow rate is assumed to be 15% greater than the amount required at the maximum power. In the final constraint management technique a predictive fuel-flow controller is added to Reference Governor B. This controller operates by first calculating the required fuel flow rate to prevent violation of the hydrogen mole fraction constraint. The procedure used for this calculation is similar to the procedure shown in Fig. 5 except that the fuel flow rate is calculated for a constant power demand. The controller then calculates the maximum feasible power with the previously calculated fuel flow as the input.

6.4. Reference governor for a realistic system

In most practical systems natural gas or other hydrocarbon fuel is typically used to provide hydrogen to the fuel cell through reformation reactions and fuel processing. In a system with natural gas reformation, dynamics associated with the reformation reactions will also be present in addition to the fluid dynamics. The use of natural gas will also affect the total flow rates and species mole fractions in the anode and cathode compartments. In an ideal situation, the hydrogen starvation problem would remain a second order problem in which case the reference governors developed for the hydrogen fueled model could be modified for use in the natural gas system. This section discusses the modifications and assumptions necessary to produce a second order reference governor when natural gas reformation is used.

The reformation dynamics can be neglected by assuming a constant molar formation rate. By assuming a steam-to-carbon ratio of two and complete conversion of the methane, the number of moles entering the volume becomes a multiple of the number of moles entering the plenum volume as follows.

$$\dot{N}_{\rm CH_4} + \dot{N}_{\rm steam} + \sum r = 5\dot{N}_{\rm CH_4} \quad (17)$$

$$\dot{P}_{\rm ref} = \frac{RT_{\rm ref}}{V_{\rm ref}}(5\dot{N}_{\rm CH_4} - \dot{N}_{\rm fc}) \quad (18)$$

where $\dot{N}_{\rm CH_4}$ is the molar flow rate of methane entering the reformer control volume and $\dot{N}_{\rm steam}$ is the molar flow rate of steam entering the reformer control volume.

When steam reformation is used, a mixture of hydrogen, steam, methane, carbon dioxide, and carbon monoxide will enter the anode instead of pure hydrogen. Since carbon monoxide and methane can be converted into hydrogen in the anode compartment, an equivalent hydrogen mole fraction can be defined to account for the potential of hydrogen production in the anode. The equivalent hydrogen mole fraction can be defined as

$$x_{\rm H_2eqv} = x_{\rm H_2} + 4x_{\rm CH_4} + x_{\rm CO} \quad (19)$$

If all of the methane and carbon monoxide are reformed into hydrogen and carbon dioxide then the equivalent hydrogen mole fraction would be achieved. Note that this variable is used only in the controller algorithm (not in fuel cell model). Using this equation results in a slight error in the predicted voltage of the control algorithm since hydrogen is assumed to be the only electrochemically active species. The anode exhaust stream typically contains a mole fraction of carbon monoxide between 2 and 3%. In order to account for this error a constant carbon monoxide mole fraction of 0.025 is assumed in the control algorithm to prevent the need to solve chemical kinetic or equilibrium equations in the reference governor model. Note that using the equivalent hydrogen mole fraction in the reference governor model also results in a more severe fuel starvation constraint since both carbon monoxide and carbon dioxide occupy space as diluents in the anode compartment, which reduces the effective hydrogen storage of the anode.

The species conservation equation can be expressed in terms of equivalent hydrogen by dividing the species conservation equation by the equivalent hydrogen mole fraction of the anode inlet stream.

$$\dot{x}_{\rm H_2eqv} = \frac{\dot{N}_{\rm fc} + r_{\rm H_2eqv} - x_{\rm H_2eqv}(\sum r + \dot{N}_{\rm fc})}{x_{\rm H_2eqv\_in} N} \quad (20)$$

In an actual system the temperatures, which were assumed constant over the time frame of concern to the reference governor model, will vary during transients and over the range of steady state operating points. In addition, the actual extent of reformation, which was assumed constant in the current analyses, will

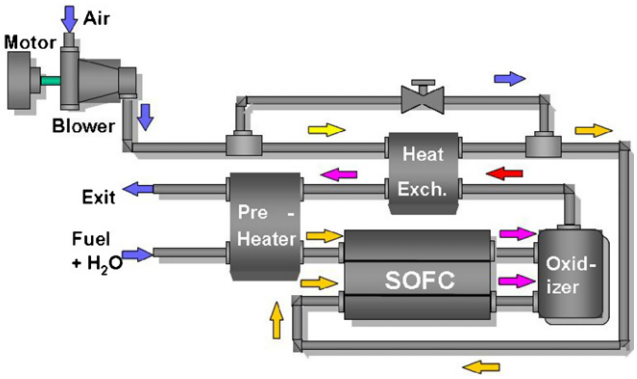

Fig. 7. Illustration of full system model.

also depend on the temperature of the reformer. These conditions will depend on the interaction of several system components. Thus, in order to test the validity of constant temperature and molar formation rate, the reference governors were tested in a model that includes the temperature dynamics and component interaction. The system configuration used in this paper is shown in Fig. 7 and includes a blower, combustor, and heat exchanger. The unutilized fuel is oxidized in a combustor. The exhaust gases of the combustor are then used to preheat the cathode inlet air. The exhaust is then used to preheat the fuel and evaporate water for the system. A bypass valve on the air pre-heater is used to maintain cathode inlet temperature within 150 degrees of the maximum fuel cell temperature. The parameters used for the complete system model are presented in Table 2.

7. Results

Different rate limiters were applied to the model for a step change from 50 to 300 kW as shown in Fig. 8. The value of the rate limiter should be chosen so that the hydrogen mole fraction will not drop below an unacceptable value for any circumstance. The rate limiter will slow the response of the system by reducing the fuel flow rate as well. Fig. 9 shows the difference in the fuel cell hydrogen flow rate when the power demand is limited

Table 2
Parameters for full system mode

Parameter	Value
Set utilization	0.85
Max utilization	0.9
Fuel cell temperature	1150 K
Anode volume	1.0×10^{-5} m^3
Reformer volume	0.5 m^3
Reformer orifice constant	1.5×106 kPa/(kmol s)^2
Number of cells	8000
Exchange current density	4000 A m^{-2}
Limiting current density	9000 A m^{-2}
Thickness of electrolyte	0.01 m
Electrolyte density	1500 kg m^{-3}
Electrolyte specific heat capacity	0.8 kJ kg^{-1} K^{-1}
Separator plate thickness	0.01 m
Separator plate density	7900 kg m^{-3}
Separator plate heat capacity	0.64 kJ kg^{-1} K^{-1}

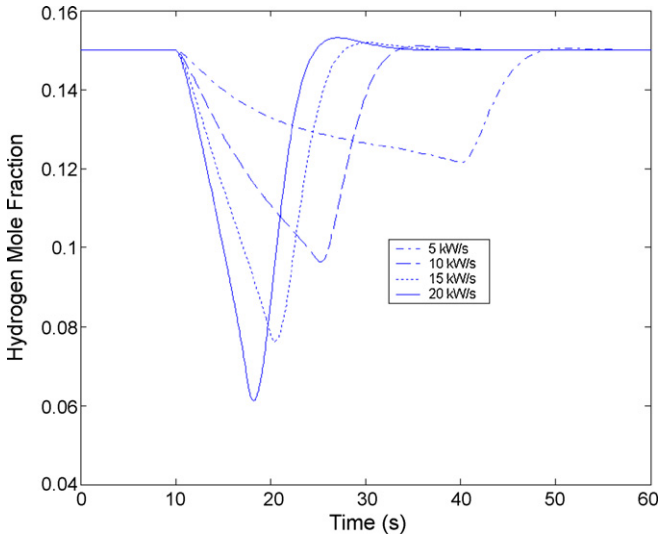

Fig. 8. Fuel cell hydrogen mole fraction for various rate limiters for a 50–300 kW step change in power demand.

by a 10 kW s^{-1} rate limiter and when the power is not limited for a step in power demand between 50 and 100 kW. A power step change from 50 to 100 kW was chosen since this is the largest step change for which a rate limiter is not needed to avoid hydrogen depletion within the fuel cell.

The SOFC system dynamic response characteristics when using (1) the first order reference governor (Governor A) based only on the reformer model, (2) the second order reference governor (Governor B) based on both the reformer and anode model, and (3) the 10 kW s^{-1} rate limiter are compared in Fig. 10. The time horizon of the second order reference governor was set to three seconds. The first order reference governor allows the power to increase slightly initially to the power that corresponds to the minimum hydrogen mole fraction for the fuel entering the fuel cell and then increases as the fuel flow to the anode increases. The second order reference governor allows the power to increase to a constant value (240 kW for this step

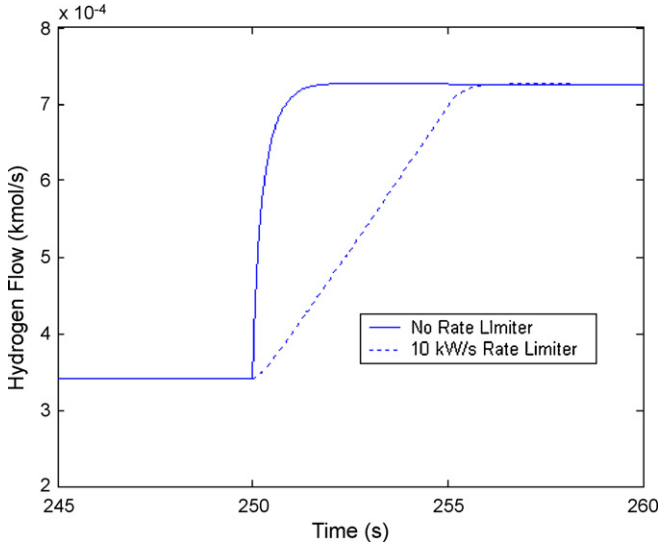

Fig. 9. Hydrogen flow rate entering fuel cell for system with and without a rate limiter for a 50–100 kW step change.

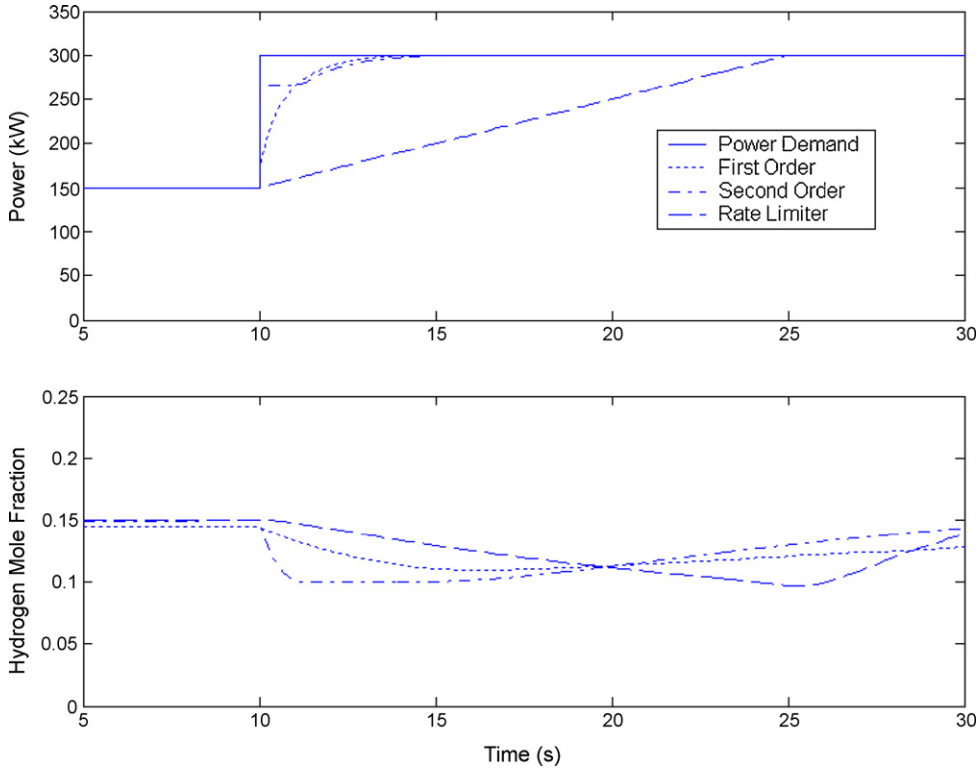

Fig. 10. Comparison of different reference governor allowable power and resulting hydrogen mole fraction.

change) until the minimum hydrogen mole fraction is reached. Governor B subsequently allows the power to increase as more fuel is added while maintaining the hydrogen mole fraction at a constant value.

One way to compare the performance of the different reference governors is in terms of the energy storage required to meet the difference between the power output and the demanded power. The $10\,\mathrm{kW\,s^{-1}}$ rate limiter would require 1000 kJ of

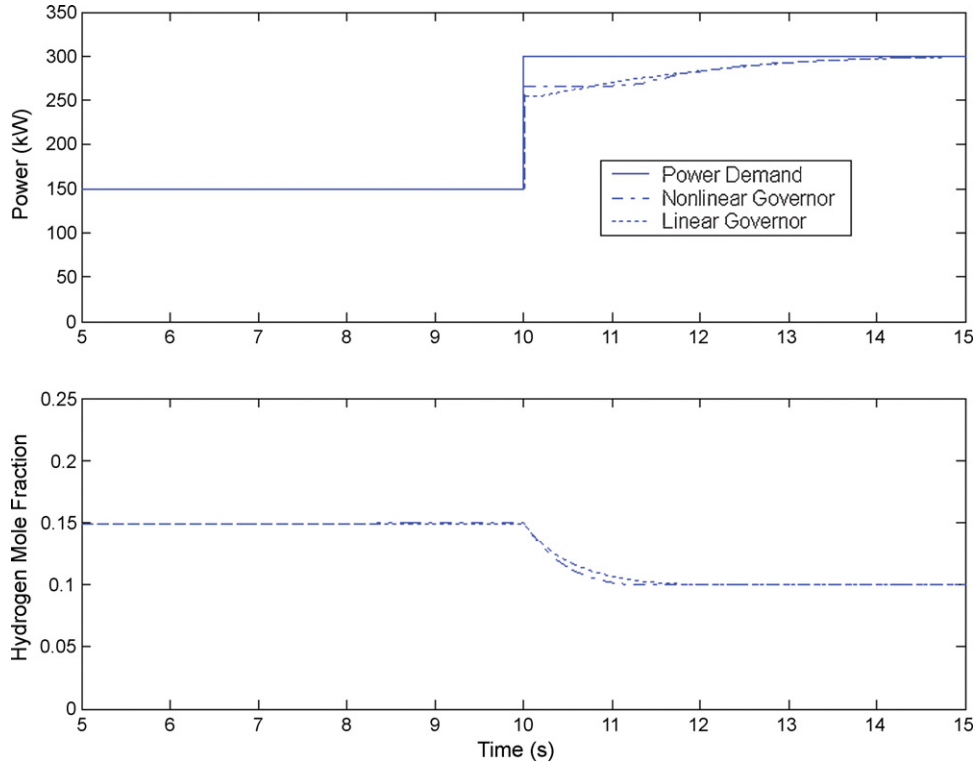

Fig. 11. Comparison of second order nonlinear and linear reference governors.

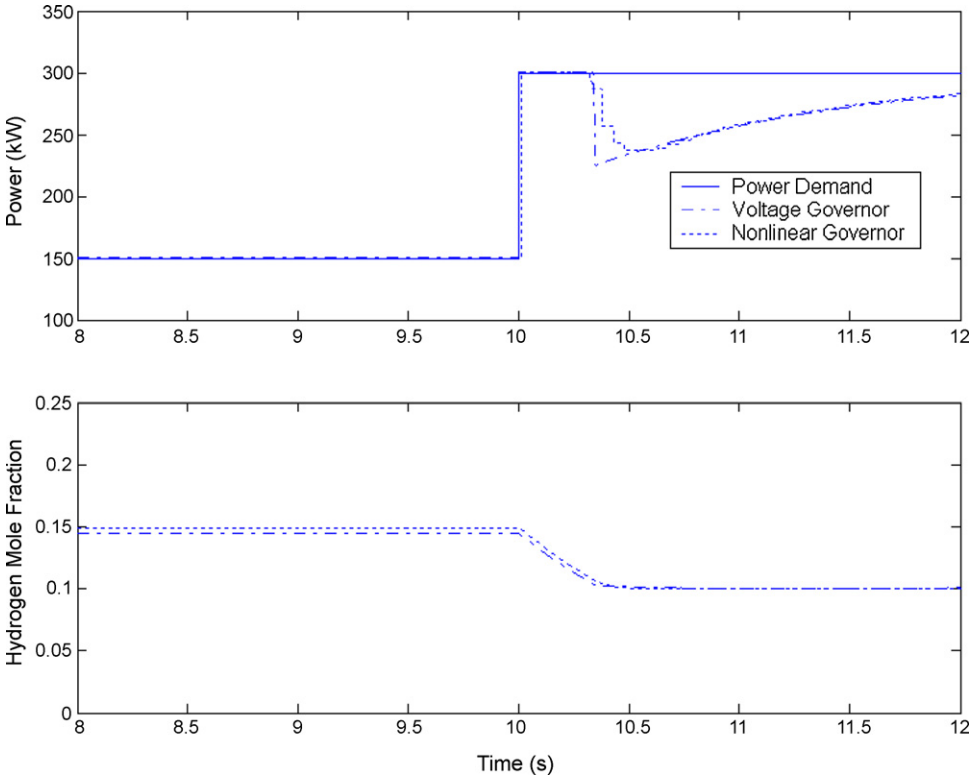

Fig. 12. Response of governor with 0.1 s time horizon and voltage-based reference governor.

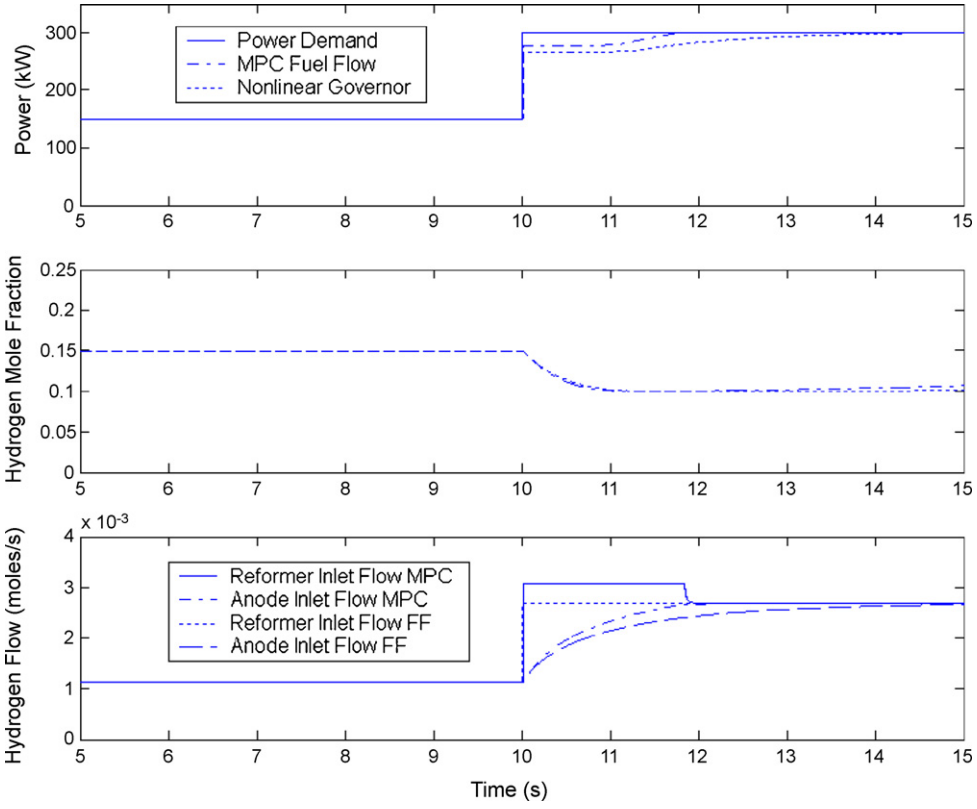

Fig. 13. Response of power, hydrogen mole fraction, and fuel flow for a 150 kW step change in power demand with the model predictive controller that can control the fuel flow rate.

Table 3
Comparison of energy storage requirements for different reference governors

Constraint management technique	Inputs	Energy storage required for 150 kW step (kJ)
Rate limiter	None	1125
First order	Fuel flow	100
Second order		
3-s time horizon	Fuel flow, estimated	82
0.1s time horizon	mole fraction	83
Fuel flow control		36
Linear		82
Voltage	Voltage	93
Second order with MPC fuel-flow controller	Fuel flow, estimated mole fraction	36

energy storage. The first order reference governor would require 100 kJ of energy storage and the second order reference governor would require 82 kJ. The second order reference governor requires approximately 20% less energy storage than the first order governor because the second order allows the reference governor to use the maximum amount of hydrogen stored in the anode since it allows the hydrogen mole fraction to reach its minimum value while the first order reference governor does not. The second order reference governor may be even more advantageous because most of the power is met initially. Therefore the stored energy maximum power (energy/time) output can be dramatically reduced.

The second order reference governor that used the nonlinear second order model is compared to that which used the linear second order model in Fig. 11. With the previously mentioned assumptions the linear model is able to perform equally as well as the nonlinear model and would also require 82 kJ of energy storage. The adjustments to the linear mode prevent the model from over predicting the allowable power output without compromising the performance of the reference governor.

When the time horizon for the second order reference governor (Governor B) is set to 0.1 s the reference governor allows the power demand to be met for about half a second before the reference governors require a reduction in the power produced. The voltage reference governor provides a similar response as shown in Fig. 12. This behavior occurs because the reference governor does not reduce the power until the hydrogen mole fraction has reached its minimum value for the voltage based governor or has nearly reached its minimum for the nonlinear governor. Energy storage of 83 kJ would be required for both of these reference governors to allow the system to

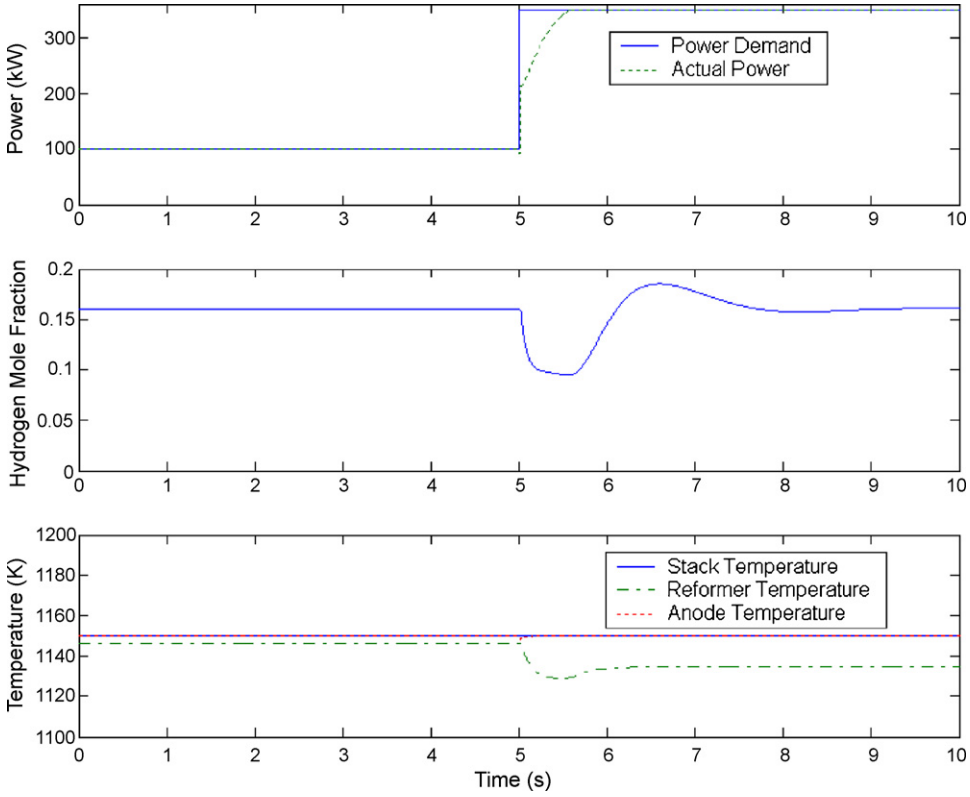

Fig. 14. Results when reference governor is used on full system.

meet this step change in power demand. However, the voltage reference governor requires significantly less computation than the nonlinear reference governor. Note that the voltage feedback reference governor performance is almost identical to the second order reference governor with a longer time horizon.

The results for the reference governor with model predictive fuel flow compensation (Governor C) for a 150 kW step increase in power demand are shown in Fig. 13. With this controller the fuel flow command saturates at its maximum value when the step change in power demand is applied to the system. When the fuel flow compensator is added, the reference governor allows the power demand to initially increase to 275 kW instead of 240 kW. The reference governor subsequently allows the power to increase as more fuel is added. The amount of energy storage required to meet the step increase in power demand is reduced to 36 kJ as compared to 82 kJ. If the maximum system fuel flow was not limited, the system power would not have to be governed at all. The results of the different reference governors considered herein are summarized in Table 3.

The system dynamic response to a step change in power demand from 100 and 350 kW for the case of a reference governor with model predictive fuel flow compensation (Governor C) are shown in Fig. 14. A larger step change is applied to demonstrate the reference governor ability to operate over a large range of operating points in a more realistic system model. Nearly all of the methane in the reformer is converted to hydrogen and carbon monoxide during the system transient. The electrolyte tri-layer and anode temperature also remain nearly constant during the time period of the transient response. The reformer temperature varies less than 25 K over the range of operation. For these conditions 62 kJ of energy storage would be required to meet the power demand. The energy storage requirement for the full system model differs from that of the simplified system since the dynamics of the reformer are different resulting in changes in molar flow rates and reaction rates as well as other system parameters.

8. Summary and conclusions

Fuel starvation is an important fuel cell system operating constraint that when violated can damage the cell. Fuel starvation can occur during rapid load increases if no action is taken to prevent it. In this paper four general methods for preventing fuel starvation were considered. Reference governors can significantly improve the performance of a solid oxide fuel cell system compared to rate limiters, which will slow the response of the system more than necessary to prevent fuel starvation. Adding an improved fuel-flow controller that will increase the fuel flow rate to compensate for the fuel flow delay can further improve the response of the system. In order for reference governor control to be effective, the controller must be able to accurately predict the response of the system and account for the hydrogen stored in the anode compartment. Such a model can be constructed from a first order fuel processor flow delay and a model of the anode hydrogen mole fraction.

References

[1] J.R. Meacham, et al., J. Power Sources 156 (2) (2006) 472–479.
[2] J. Sun, I.V. Kolmanovsky, IEEE Trans. Control Syst. Technol. 13 (6) (2005) 911–920.
[3] A. Vahidi, I. Kolmanovsky, A. Stefanopoulou, Proceedings of the American Control Conference, 2005.
[4] C. Stiller, et al., J. Power Sources 141 (2) (2005) 227–240.
[5] C. Stiller, B. Thorud, O. Bolland, J. Eng. Gas Turbines Power 128 (2006) 551–559.
[6] F. Mueller, et al., J. Power Sources 172 (1) (2007) 308–323.
[7] P. Beckhaus, et al., J. Power Sources 127 (1/2) (2004) 294–299.
[8] V. Tsourapas, A. Stefanopoulou, J. Sun, Am. Control Conf. 3 (2005) 1993–1998.
[9] A. Vahid, A. Stefanopoulou, H. Peng, Proceedings of the American Control Conference, 2004.
[10] E. Gilbert, I. Kolmanovsky, Int. J. Robust Nonlinear Control 9 (1999) 1117–1141.
[11] F. Mueller, Design and Simulation of A Tubular Solid Oxide Fuel Cell System Control Strategy, in Mechanical and Aerospace Department, University of California, Irvine, Irvine, 2005, p. 141.
[12] R.A. Roberts, J. Brouwer, ASME J. Fuel Cell Sci. Technol. 3 (1) (2006) 18–25.
[13] R. Roberts, A Dynamic Fuel Cell-Gas Turbine Hybrid Simulation Methodology to Establish Control Strategies and an Improved Balance of Plant, in Mechanical and Aerospace, University of California, Irvine, Irvine, 2005, p. 338.
[14] F. Mueller, et al., ASME J. Fuel Cell Sci. Technol. 3 (2) (2006) 144–154.
[15] J. Brouwer, et al., J. Power Sources 158 (1) (2006) 213–224.
[16] F. Mueller, et al. Linear Quadratic Regulator for a Bottoming Solid Oxide Fuel Cell Gas Turbine Hybrid System. ASME Paper ICEPAG2006-24018, Newport Beach, CA, 2006.
[17] R. Roberts, J. Brouwer, ASME J. Fuel Cell Sci. Technol. 3 (2006) 18–25.
[18] K. Min, et al., Dynamic Simulation of a Stationary PEM Fuel Cell System, ASME Paper FC2006-97039, Irvine, CA, 2006.
[19] F. Mueller, et al., ASME J. Fuel Cell Sci. Technol. (2007).
[20] T. Kaneko, J. Brouwer, G.S. Samuelsen, J. Power Sources 160 (1) (2006) 316–325.
[21] F. Mueller, et al., J. Power Sources 176 (1) (2008) 229–239.
[22] R. Kandepu, et al., Energy 32 (4) (2007) 406–417.
[23] J. Xu, G.F. Froment, AIChE 35 (1) (1989) 97–103.
[24] J. Xu, G.F. Froment, AIChE 35 (1) (1989) 88–96.